# A new direct yaw moment control with lateral forces effect consideration

**S. H. Tabatabaei Oreh[1], R. Kazemi[2], N.Esmaeili[3]**

1- Department of Mechanical Engineering, Islamic Azad University South Branch of Tehran, Tehran, Iran 2- Department of Mechanical Engineering, K. N. Toosi University of Technology, Tehran, Iran 3- Department of Mechanical Engineering, K. N. Toosi University of Technology, Tehran, Iran

* nesmaeili@mail.kntu.ac.ir

**Abstract**

Direct Yaw moment Control systems (DYC) can maintain the vehicle in the driver's desired path by distributing the asymmetric longitudinal forces and the generation of the Control Yaw Moment (CYM). In order to achieve the superior control performance, intelligent usage of lateral forces is also required. The lateral wheel forces have an indirect effect on the CYM and based upon their directions, increase or decrease the amount of CYM magnitude. In this paper, a systematic and applicable algorithm is proposed to use the lateral force in the process of Yaw controlling optimally. The control systems are designed based on the proposed algorithm. This system includes Yaw rate controller and wheel slip controllers which are installed separately for each wheel. Both of the mentioned control systems are designed on the basis of the Fuzzy logic. Finally, the capabilities of the proposed control systems are evaluated in a four wheel drive vehicle, for which, the traction of each wheel can be controlled individually. It is shown that considering the lateral force effect offers significant improvement of the desired yaw rate tracking

***Keywords****: Yaw rate control; Wheel slip ratio; Fuzzy logic; Control yaw moment; Lateral force;*

## 1. Introduction

One of the most important safety factors in vehicle is its predictable and stable behavior. The vehicle which is moving on slippery roads does not properly respond to the drivers command and its behavior is not predictable since the quick saturation of lateral forces is involved. In this case, vehicle handling behavior is not predictable, and vehicle becomes less responsive to the driver steering input. As a result, various active safety control systems have been actively studied and developed in the last three decade, including Active Front Steering system (AFS), Rear Wheel Steering system (RWS), 4 Wheel Steering system (4WS), and Direct Yaw moment Control system (DYC) which are currently being used in the market.

In these systems, Yaw rate and/or side slip angle are regarded as the control variables. The DYC system which is also known as ESP, VDC and etc is the most outstanding sample among the mentioned systems. This system controls the Yaw rate and/or side slip angle through the asymmetric distribution of longitudinal forces. This approach was first suggested by Matsumoto et al. [1] and then was developed by many other researchers [2-5].

The researches on the development of the active safety systems can be categorized as follows: Some of them have considered the Yaw rate as the main control variable and adjusted the Yaw rate using DYC systems [6,7]. Some others have only considered the side slip angle as control variable and have developed the DYC system in order to adjust it [8,9]. Another category controls both Yaw rate and side slip angle using one control input [10-13]. Here it is important to note that from the theoretical point of view, the simultaneous controlling of two variables requires the application of two control inputs [14,15]. Many researchers have considered this point and have applied the DYC system in an integrated way with different kinds of other active safety systems such AFS [16-18]. But, we should bear in mind that the deviation of side slip angle from the permitted

boundaries occurs most often in low friction coefficient. Considering the tire behavior, the lateral wheel forces are saturated quickly on such roads. Consequently on slippery roads, active safety systems which use the lateral forces in vehicle controlling, can not be relied upon to be used as helping systems to DYC. Therefore, the simultaneous yaw rate and side slip angle controlling on low friction coefficient roads is still regarded as a challenging task.

In this paper, the DYC system has been specifically designed to adjust the vehicle yaw rate. On the other hand, the tire capacity to generate the control yaw moment has been increased by continuous attempts.

Recently, optimizing tire usage has been brought about as a necessity and has attracted many researchers including: Peng and Hu proposed an algorithm for the optimal distribution of longitudinal forces to obtain maximum acceleration and deceleration [19]. Tavasoli and Naraghi presented an optimum tire force distribution method in order to optimize tire usage and found out how the tires should share longitudinal and lateral forces to achieve a target vehicle response [20].

It has been noted that the DYC system can oriented the direction of the vehicle to the driver's desired direction using asymmetric longitudinal force distribution on the sides of the vehicle and the generation of the Control Yaw Moment (CYM). As a result, the longitudinal wheel forces are the essential means in the process of yaw control. Note that the lateral wheel forces have an indirect effect on the CYM and based upon their direction, increase or decrease the amount of CYM magnitude. We can neglect the above mentioned fact on dry roads but it can not be ignorable any more on slippery roads. On low friction coefficient surfaces, the dynamic power of the vehicle to generate the CYM is limited. Therefore, in these situations, the control system must be capable to utilize the maximum capability of vehicle to generate the yaw moment. Consequently, an appropriate control system needs to handle the lateral force effect on the CYM. However, in the previous researches, this fact has not been considered appropriately.

Therefore, in this paper a systematic and applicable algorithm is proposed to use the lateral force in the process of Yaw controlling optimally. The fuzzy control systems are designed based on the proposed algorithm and finally the capabilities of the proposed control systems is evaluated in a four wheel drive vehicle.

One of the most important safety factors in vehicle is its predictable and stable behavior. The vehicle which is moving on slippery roads does not properly respond to the drivers command and its behavior is not predictable since the quick saturation of lateral forces is involved. In this case, vehicle handling behavior is not predictable, and vehicle becomes less responsive to the driver steering input. As a result, various active safety control systems have been actively studied and developed in the last three decade, including Active Front Steering system (AFS), Rear Wheel Steering system (RWS), 4 Wheel Steering system (4WS), and Direct Yaw moment Control system (DYC) which are currently being used in the market.

In these systems, Yaw rate and/or side slip angle are regarded as the control variables. The DYC system which is also known as ESP, VDC and etc is the most outstanding sample among the mentioned systems. This system controls the Yaw rate and/or side slip angle through the asymmetric distribution of longitudinal forces. This approach was first suggested by Matsumoto et al. [1] and then was developed by many other researchers [2-5].

The researches on the development of the active safety systems can be categorized as follows: Some of them have considered the Yaw rate as the main control variable and adjusted the Yaw rate using DYC systems [6,7]. Some others have only considered the side slip angle as control variable and have developed the DYC system in order to adjust it [8,9]. Another category controls both Yaw rate and side slip angle using one control input [10-13]. Here it is important to note that from the theoretical point of view, the simultaneous controlling of two variables requires the application of two control inputs [14,15]. Many researchers have considered this point and have applied the DYC system in an integrated way with different kinds of other active safety systems such AFS [16-18]. But, we should bear in mind that the deviation of side slip angle from the permitted boundaries occurs most often in low friction coefficient. Considering the tire behavior, the lateral wheel forces are saturated quickly on such roads. Consequently on slippery roads, active safety systems which use the lateral forces in vehicle controlling, can not be relied upon to be used as helping systems to DYC. Therefore, the simultaneous yaw rate and side slip angle controlling on low friction coefficient roads is still regarded as a challenging task.

In this paper, the DYC system has been specifically designed to adjust the vehicle yaw rate. On the other hand, the tire capacity to generate the control yaw moment has been increased by continuous attempts.

Recently, optimizing tire usage has been brought about as a necessity and has attracted many researchers including: Peng and Hu proposed an

algorithm for the optimal distribution of longitudinal forces to obtain maximum acceleration and deceleration [19]. Tavasoli and Naraghi presented an optimum tire force distribution method in order to optimize tire usage and found out how the tires should share longitudinal and lateral forces to achieve a target vehicle response [20].

It has been noted that the DYC system can oriented the direction of the vehicle to the driver's desired direction using asymmetric longitudinal force distribution on the sides of the vehicle and the generation of the Control Yaw Moment (CYM). As a result, the longitudinal wheel forces are the essential means in the process of yaw control. Note that the lateral wheel forces have an indirect effect on the CYM and based upon their direction, increase or decrease the amount of CYM magnitude. We can neglect the above mentioned fact on dry roads but it can not be ignorable any more on slippery roads. On low friction coefficient surfaces, the dynamic power of the vehicle to generate the CYM is limited. Therefore, in these situations, the control system must be capable to utilize the maximum capability of vehicle to generate the yaw moment. Consequently, an appropriate control system needs to handle the lateral force effect on the CYM. However, in the previous researches, this fact has not been considered appropriately.

Therefore, in this paper a systematic and applicable algorithm is proposed to use the lateral force in the process of Yaw controlling optimally. The fuzzy control systems are designed based on the proposed algorithm and finally the capabilities of the proposed control systems is evaluated in a four wheel drive vehicle.

## 2. Dynamic Modeling

### 2.1. Vehicle model

The vehicle model used in this paper is a 14 DOF model shown in Fig. 1. Six degrees out of the 14 DOF are devoted to the sprung mass and the remaining 8 degrees belong to wheel rotation speed and unsprung masses vertical displacement.

The equations of motion for this model are derived as:

**Longitudinal motion**

$$m_t(\dot{u} + qw - rv) = F_{pfr} + F_{pfl} + F_{prr} + F_{prl} \quad (1)$$

**Lateral motion**

$$m_t(\dot{v} + ru - pw) = F_{hfr} + F_{hfl} + F_{hrr} + F_{hrl} \quad (2)$$

**Vertical motion**

$$m_s(\dot{w} + pv - qu) = F_{zfr} + F_{zfl} + F_{zrr} + F_{zrl} \quad (3)$$

**Roll motion**

$$I_{sxx}\dot{p} + (I_{szz} - I_{syy})qr = (F_{zfr} - F_{zfl})\frac{T_f}{2} + (F_{zrr} - F_{zrl})\frac{T_r}{2} - (F_{hfr} + F_{hfl} + F_{hrr} + F_{hrl})h$$

**Pitch motion**

$$I_{syy}\dot{q} + (I_{sxx} - I_{szz})pr = (F_{zrr} + F_{zrl})L_r - (F_{zfr} + F_{zfl})L_f + (F_{pfr} + F_{pfl} + F_{prr} + F_{prl})h$$

**3. Yaw motion**

$$I_{zz}\dot{r} + (I_{yy} - I_{xx})pq = (F_{pfl} - F_{pfr})\frac{T_f}{2} + (F_{prl} - F_{prr})\frac{T_r}{2} + (F_{hfl} + F_{hfr})L_f - (F_{hrr} + F_{hrl})L_r + M_{zfr} + M_{zfl} + M_{zrr} + M_{zrl} \quad (6)$$

Where $p$ is the roll rate ($\dot{p}$), $q$ is the pitch rate ($\dot{q}$) and $r$ is the Yaw rate ($\dot{r}$). The terms $F_{pi}$ and $F_{hi}$ are the respective tire forces in the $x$ and $y$ directions, which can be related to the longitudinal

$$\begin{Bmatrix} F_{pi} \\ F_{hi} \end{Bmatrix} = \begin{bmatrix} \cos d_i & -\sin d_i \\ \sin d_i & \cos d_i \end{bmatrix} \begin{Bmatrix} F_{xi} \\ F_{yi} \end{Bmatrix}$$

with $i = fr, fl, rr, rl$ (7)

and the lateral tire forces:

The steer angle of the $i^{th}$ wheel $d_i$ is assumed to have the following relationships:

$$d_{fr} = d_{fl} = d_f, \qquad d_{rr} = d_{rl} = 0 \quad (8)$$

The rotational motion of each wheel is represented as:

$I_w\dot{w}_i = T_{Ni} - F_{xi}R_{effi}$ With

$i = fr, fl, rr, rl$ (9)

The equations of motion for the suspension model are derived from Fig. 1(b) as follow:

$m_{ui}\ddot{Z}_{ui} = F_{zti} - F_{zi}$ With

$i = fr, fl, rr, rl$ (10)

Where

$F_{zi} = K_{si}(Z_{ui} - Z_i) + C_{si}(\dot{Z}_{ui} - \dot{Z}_i)$ With

$i = fr, fl, rr, rl$ (11)

$F_{zti} = K_{ti}(Z_{si} - Z_{ui}) + C_{ti}(\dot{Z}_{si} - \dot{Z}_{ui})$

With

$i = fr, fl, rr, rl$ (12)

And

$$z_{fr} = z_{CG} + \frac{T_f}{2} j - L_f q \quad (13)$$

$$z_{fl} = z_{CG} - \frac{T_f}{2} j - L_f q \quad (14)$$

$$z_{rr} = z_{CG} + \frac{T_r}{2} j + L_r q \quad (15)$$

$$z_{rl} = z_{CG} - \frac{T_r}{2} j + L_r q \quad (16)$$

### 2.2. Tire model

A part from aerodynamic forces, all the forces influencing the vehicle are created on the contact surface between the tire and the road. Hence, in the vehicle dynamic behavior simulation, the nonlinear tire behavior is considered as one of the most effective factor. Consequently, in this paper, the 2002 magic formula model version as the most perfect tire model has been used [21]. In this model, the combined slip situation was modeled from a physical viewpoint.

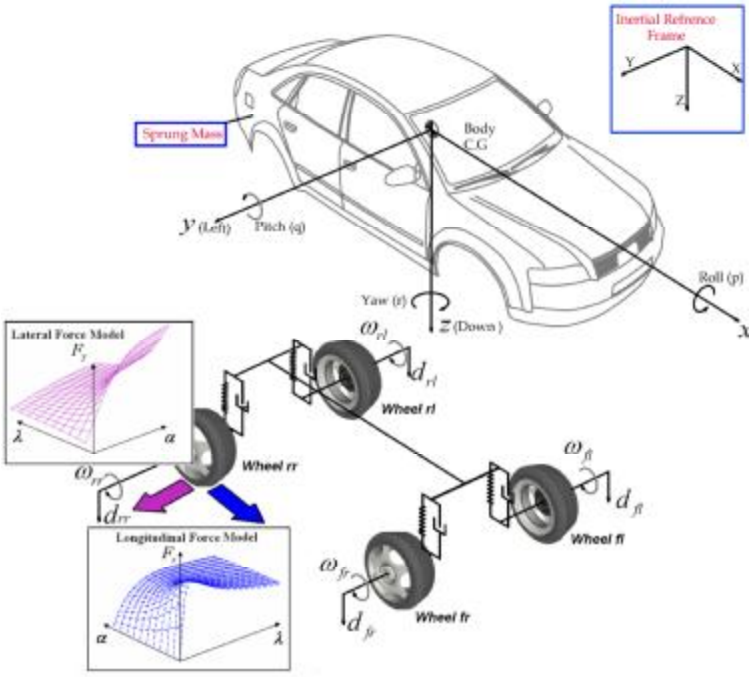


**Fig1.** Vehicle and tire model

## 2.3. Driver Model

Active safety systems are continuously involved with the driver and the general vehicle performance is not only reliant on the active safety system design but also on its interaction with the driver. On the other hand, no equation can visualize the human brain complexity. However, some researchers have proposed driver models. It seems that the preview tracking model [22] is more similar to what happen in reality. Therefore, this model is used in this paper to evaluate the control systems performance in an exact and doubtless manner. Based on the schematic of the maneuver task geometry which is shown in Fig.2(a), the following equation has been extracted for the driver applying steering angle:

$$d_f(t) = \{ \frac{K_{steer}}{L_a} [y_d(t + \frac{L_a}{V_x}) - y(t)] - K_{steer} \Psi(t) \} e^{-st_d} \quad (17)$$

According Eq.1 the above model is described through three parameters: Distance to target point $L_a$, steer angle gain $K_{steer}$ and delay time $t_d$. In this paper, the delay time is considered as a fixed parameter and its amount as reflecting the conducted research is 0.2[23]. The main issue in this model is the determination of $L_a$ and $K_{steer}$ which lead to an optimization problem. The performance index of the optimization problem is defined in proportion to the

requirement while driving and by considering dominate physical limitations as reflected in Eq. 18.

$$PI = \int_0^{t_f} (q_1 y_e^2 + q_2 d_f^{\ 2} + q_3 \dot{d}_f^{\ 2}) dt \quad (18)$$

As a result the aim of solving the problem is to find $L_a$ and $K_{steer}$ to minimize the $PI$. In Eq.18 $y_e$ indicated deviation from the desired path and is certainly the most important term of the Performance Index. So $q_1$ weights more than the other two parameters. The second term of the Performance Index somehow portray the driver's physical activity while driving. Adding the preceding term to the target function causes the steering wheel angle to be accessible. The third term of the target function both indicates the driver's mental activity and leads to the generation of a moderate curve for the steer angle.

To complete the optimization problem, it is required to define a constraint. Considering the driver limited eyesight, for $L_a$ the following constraint is proposed

$$L_a < 20m \quad (19)$$

To solve the above problem, it is necessary to define a desired path. In this paper double lane change maneuver according to standard No. ISO/TR 3888:1975 has been selected. To find the unknown parameters, the genetic algorithm is used. In Fig.2 (b) the block diagram of the optimization problem has been shown.

The results read as follows:

$K_{steer} = 0.385, L_a = 19.169$

In the simulation section, the driver's response is evaluated with and without control.

### 2.4 Model Validation

The dynamic responses of the vehicle model that include yaw rate, side slip angle and roll angle can be validated using experimental results which are available in Ref. [24]. Comparisons between simulation responses of the developed model and test results for the double lane change manoeuvre conducted at 80 km/h are shown in Figure 3. Clearly, the responses of the model exhibit well match with the test result.

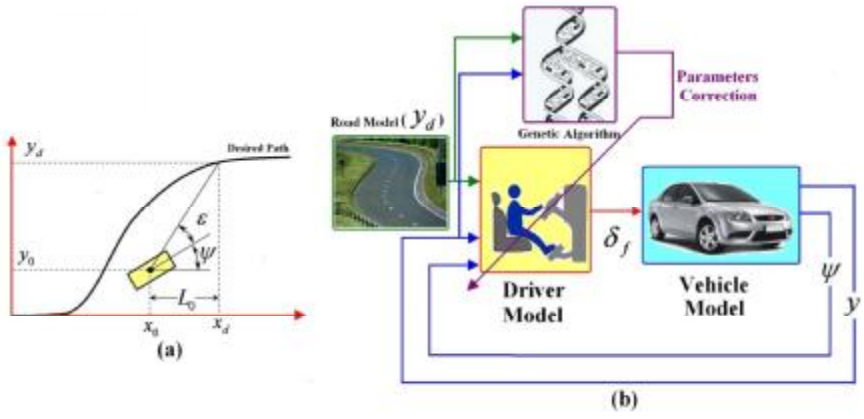


**Fig2.** (a)Geometry of desired path tracking by driver (b) Block diagram of the driver Model parameters identification

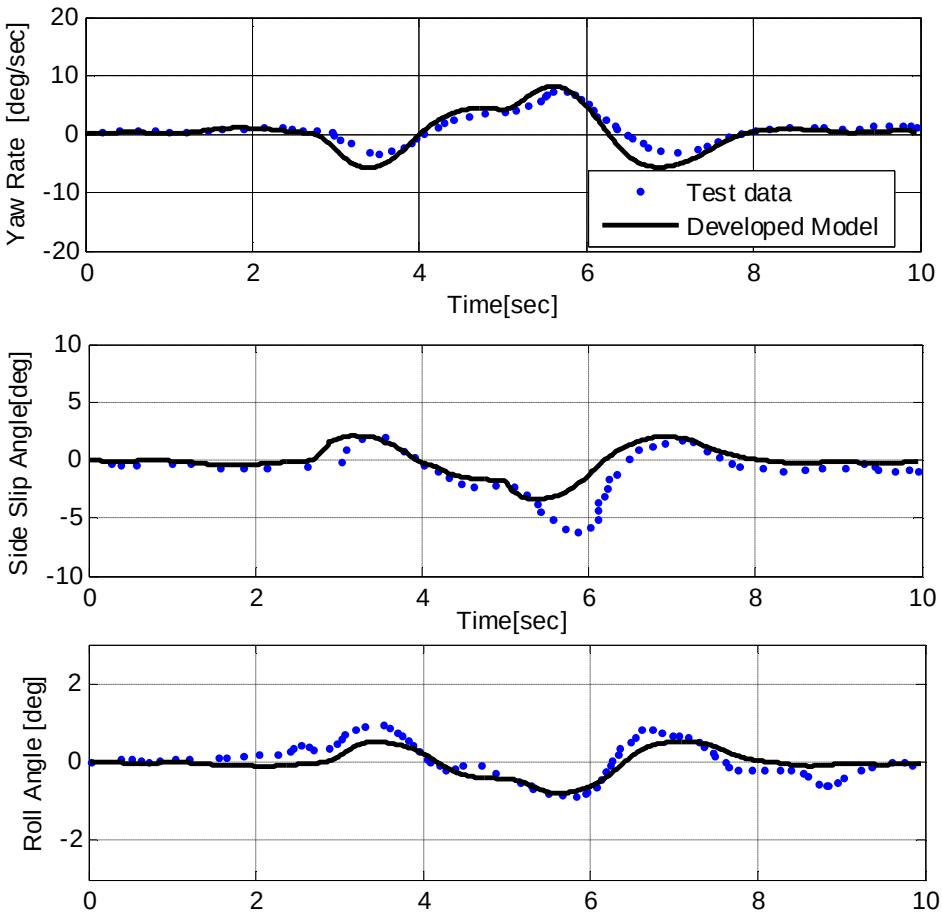


**Fig3.** Model validation results

## 3. Physical Consideration

### 3.1Yaw rate control through the longitudinal forces

In vehicle lateral motion control, vehicle yaw rate is known as one of the most important variable. There is a desired amount for this variable the approximation of which equals the provision of the desired behavior expected by the driver. Hence the aim of the control system is to minimize the error between the yaw rate $(r)$ and desired amount $(r_d)$. The variable $r_d$ as reflecting Eq.(20) is defined based on the driver's steer angle $(d_f)$ and longitudinal velocity $(V_x)$.

$$r_d = \frac{V_x}{L(1+\frac{K_{us}}{L}V_x^2)}d_f \qquad (20)$$

Vehicle yaw control system makes the yaw rate closer to its desired value through asymmetric longitudinal force distribution. Consequently a Control Yaw Moment (CYM) is generated and the vehicle is oriented toward the desired direction. In Fig.(4), a vehicle in over steer situation is shown. In this figure, the forces applied to the vehicle during the control system activation are schematically depicted.

Clearly, the further the distance of yaw rate from its desired value, a bigger control yaw moment is required. Therefore the control system applies more traction/braking torque to the wheels as the error amount increases so that the increasing of slip ratio causes a larger longitudinal force and leads to stronger control yaw moment. But, taking the following point into account is of importance:

According to Fig.5 (a), because of the nonlinear nature of the tire, when the tire reaches the point $l_{\max}$, the increased applied torque to the tire does not enlarge the longitudinal force and therefore the

control system gains a reverse conclusion. Consequently the control system must be designed in a way that restricts the applied torque to the tire after the diagnosis of the above mentioned circumstances and cause the tire not to enter the area with the descending slope of the longitudinal force.

Of course, $|l| < l_{max}$, has been regarded as the stable area of operation and the maintaining of the wheel slip ratio in this region has been brought about as one of the main principles. To meet this important demand, two main approaches are taken into consideration. In some researches, slip ratio controllers are installed for each wheel to maintain the slip ratio of the wheel in the stable region [25]. In some other systems, a specific bound for the traction/ braking torque has been considered so that the applied torque to the wheels is not allowed to depart [16]. In this case, the latter approach does not seem very exact.

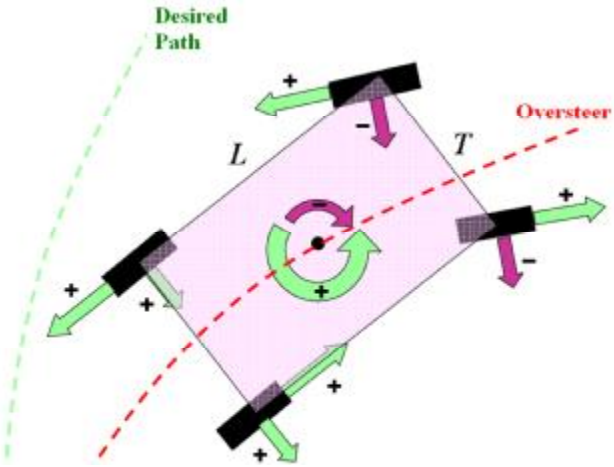


**Fig4.** Schematic of forces applied to the vehicle during the control system activation

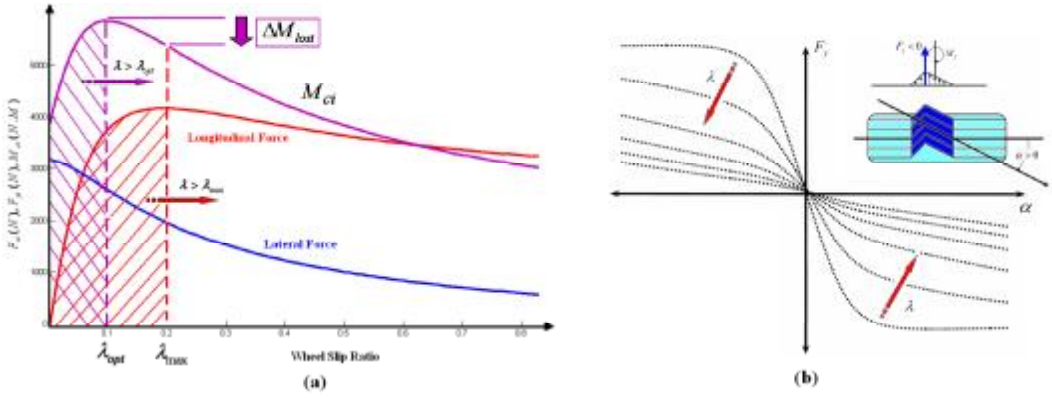


**Fig5.** (a)longitudinal force $(F_{xi})$, lateral force $(F_{yi})$ and the defined moment $(M_{ci})$ respect to wheel slip ratio, (b) Tire lateral force respect to wheel slip angle

### 3.2 Yaw Rate Control as Considering The Lateral Forces Effect

In the previous section, the nonlinear shape of the longitudinal force was considered to be one of the main principles in the Yaw rate controlling. The important point which has not been seriously

considered is that the lateral force has an indirect effect on the CYM and depending on its direction, increases or decreases the CYM. This fact in ideal conditions such as driving on a dry road is negligible but cannot be ignored on slippery roads. The less the road friction coefficient, the less the dynamic power of the vehicle in generating CYM. In this situation, the control system should be designed in such a way that makes the most usage of the vehicle dynamic capacity.

According to Fig.4, depending on the lateral force direction, it increase or decreases the CYM. The direction and magnitude of the lateral force relies on the wheel slip angle as shown in Fig.5(b). In Fig.4, for all wheels the slip angle was supposed to be negative. The positive/negative definition of the slip angle is carried out based on the SAE standard. In addition, the traction-braking torque applied to the wheels through the control system has an effect on the lateral force from a quantitative perspective. Hence, as shown in Fig.5(b), through the application of this torque and the increasing of wheel slip ratio, the lateral force is decreased.

The above mentioned points are used in investigating an approach to the appropriate distribution of the traction/braking torque on the wheel. For this purpose, CYM ($M_c$) is decomposed as follows:

$$M_c = M_{cfr} + M_{cfl} + M_{crr} + M_{crl} \tag{21}$$

That $M_{ci}$ $(i = fr, fl, rr, rl)$ indicates the share for each wheel in $M_c$ generation. Considering the steer wheel angle and self-aligning torque as small in amount, and also placing the center of gravity on the geometric center, we can come up with the following $M_{ci}$ general equation:

$$M_{ci} = +F_{xi}\frac{T}{2} \pm F_{yi}\frac{L}{2} \tag{22}$$

Bear in mind that the positive/negative signs in Eq.22 are not defined in relation to any coordinate system but are respectively indicative of the increasing/decreasing effect of the forces on the CYM. Therefore the longitudinal force is shown by the positive sign and the lateral force dependent on slip angle appears with the positive or negative sign. Based on Eq.22 the two following situations are defined while the consideration of them leads to the extraction of optimal control strategies:

**Situation 1: Lateral Wheel Force with Positive Effect on CYM**

The following relation is the dominate equation in this situation. Here the lateral force maintains the CYM.

$$M_{ci} = +F_{xi}\frac{T}{2} + F_{yi}\frac{L}{2} \tag{23}$$

Now, the question is how to make an optimal decision?

In answering this question, we should be aware that the control system conducts its responsibilities through CYM generation. Therefore, the optimal decision is the maintenance of slip ratio in the $M_{ci}$ ascending band not in the longitudinal force ascending band proposed in section (3-1). In Fig. 4(a), longitudinal force $(F_{xi})$, lateral force $(F_{yi})$ and the defined moment in Eq.23 $(M_{ci})$ are depicted as a function of $l$. The maximum CYM is generated in the optimal slip ratio$(l_{opt})$. In other words, increasing $l$ to $l_{\max}$leads to the lose of generated yaw moment with the amount of $\Delta M_{lost}$. Hence the control system must be designed in a way that maintains the slip in $|l| < l_{opt}$ area if the positive effect of lateral force on the control process is diagnosed. We should consider that the decreasing of road surface friction coefficient causes the $l_{opt}$ to be moved and get closer to zero. Consequently the amount of $l_{opt}$ in different road friction coefficients is determined and registered in Table 1.

**Table 1:** Optimum wheel slip ratio in different road conditions

| $m$ | 0.1 | 0.2 | 0.3 | 0.4 | 0.5 | 0.6 | 0.7 | 0.8 | 0.9 | ١ |
|---|---|---|---|---|---|---|---|---|---|---|
| $l_{opt}$ | 0.02 | 0.03 | 0.04 | 0.05 | 0.06 | 0.07 | 0.08 | 0.10 | 0.11 | 0.12 |

**Situation 2. Lateral Wheel Force with Negative Effect on CYM**

The dominate equation for this situation is defined based on the following Eq.24.

$$M_{ci} = +F_{xi}\frac{T}{2} - F_{yi}\frac{L}{2} \quad (24)$$

The control approach is to decrease the amount of the negative term (lateral force) remarkably. This idea equals the increasing of the slip ratio to the spinning or locking area. The above mentioned statement is rejected from a practical viewpoint and is in contrast to the main governing constraint. (Slip maintenance in the stable region is the main governing constraint). In this situation, the slip controller of each wheel allows $l$ to reach boundary of the stable region $(l_{\max})$, if it diagnoses the negative effect of the lateral force on CYM.

### 3.3. Switching Function

Based on the conducted analysis, it is necessary to define a new parameter for the distinction of the lateral force effect on the CYM. To reach this aim, all possible situations should be carefully studied and comprehensive approach should be extracted as reflecting the observation. In Fig.6, all possible situations as related to the turning motion and the control system activation are depicted. These situations are divided on the basis of positive or negative $\Delta T$. According to this figure in each situation the lateral force of each wheel is depicted on both possible directions to cover all the probabilities.

The switching function $h$ is introduced as Eq.25 after the close examination of the situation include in Fig. 6,

$$h_i = \Delta T.a_i \quad (25)$$

In this equation $a_i$ indicates slip angle of $i^{th}$ wheel and $\Delta T$ is the output of the yaw rate controller. Based on the following model the positive or negative effect of the lateral force on the CYM is recognized as reflecting the positive or negative sign of the switching function:

I. In front wheels $(i = fr, fl)$:

If we have $h_i > 0_i \quad (h_i < 0_i)$ so the result is decreasing (increasing) the CYM

II. In rear wheels $(i = rr, rl)$:

If we have $h_i < 0_i \, (h_i > 0_i)$ so the result is decreasing (increasing) the CYM

Therefore the switching function is defined as a new input for the control system. According to the analysis, the permitted region of the slip ratio for each wheel is determined based on the $h$ sign. In addition the friction coefficient must also be included in the definition of this region.

### 4. Control System Design

Based on the preceding material, the structure of the proposed control system is chosen according to Fig.7. This system includes Yaw rate controller, wheel slip controllers which are installed separately for each wheel. Both of the mentioned control systems are designed on the basis of the Fuzzy logic.

The aim of the Yaw rate controller is to reduce the error between Yaw rate and its desired value. The output of this controller is the differential torque applied to the wheels. Then through the activation of the control system the longitudinal forces of both sides of the vehicle are generated in opposite direction. The final result of these forces is the CYM which minimizes the Yaw rate error. According to the principles in section 3, the slip controller maintains the slip ratio in the region where the CYM can be maximized.

### 4.1Yaw Rate Controller Design

This controller adjusts the vehicle Yaw rate through corrective yaw moment generation by distributing the traction and braking forces on the wheels. Yaw rate error is defined according to Eq. 26.

$$e_r = r_d - r \quad (26)$$

Quantity $e_r$ and its derivation $\dot{e}_r$ are defined as the control system inputs. The output of this controller is the differential torque $\Delta T$ applied to the wheels. The rule based of this controller is shown in Table 2. By using the input and output scaling factor defined for $e_r$ and $\dot{e}_r$, all the membership functions related to $e_r$, $\dot{e}_r$ and $\Delta T$ have been normalized between [-1 1]. The input and output scaling factors are selected as considering dynamic system limitations and trial and error to reach the most desired performances.

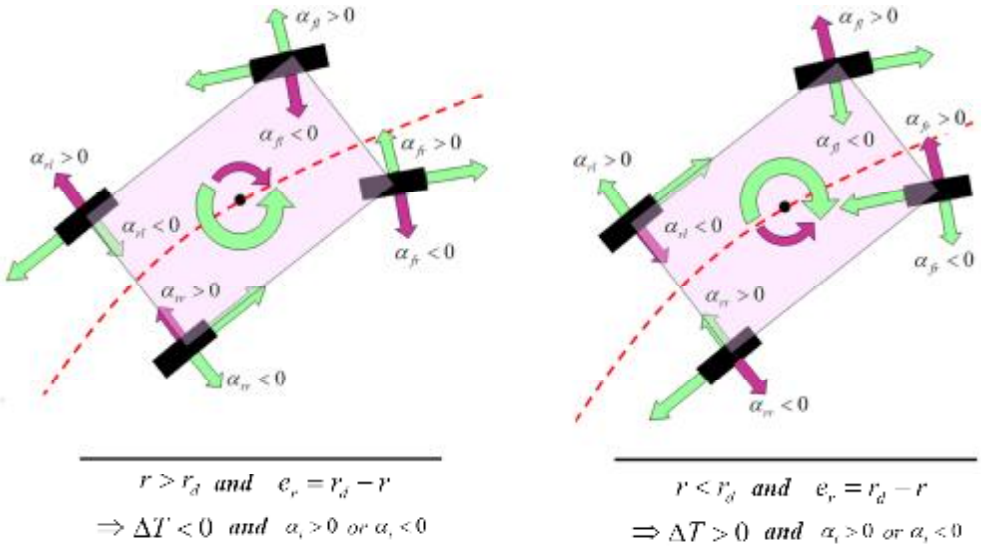


**Fig6.** Two general situations in vehicle cornering during activation of the control system

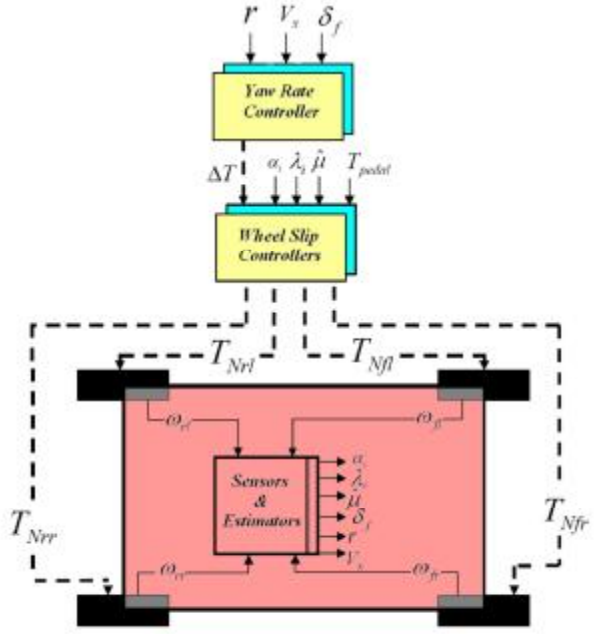


**Fig7.** Block diagram of the proposed DYC system

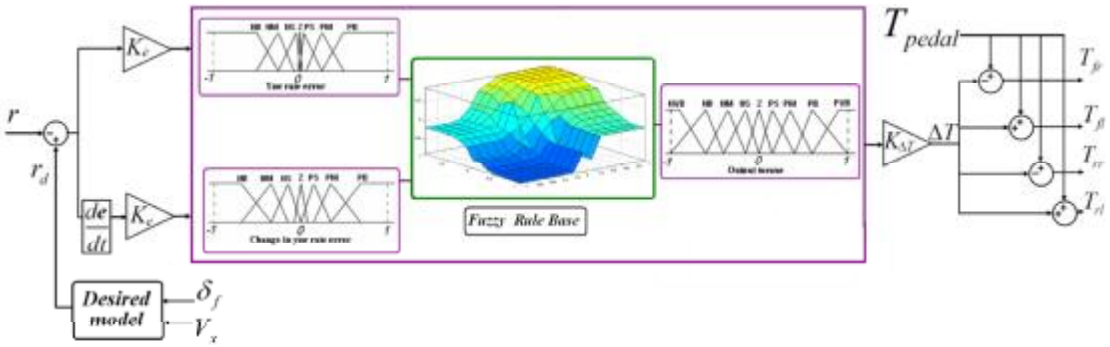


**Fig8.** Fuzzy logic yaw rate controller

**Table 2:** Fuzzy rules for yaw rate fuzzy controller

| | Error | | | | | | |
|---|---|---|---|---|---|---|---|
| | **NB** | **NM** | **NS** | **Z** | **PS** | **PM** | **PB** |
| **Derror** | | | | | | | |
| **NB** | NVB | NVB | NVB | NM | NB | Z | Z |
| **NM** | NVB | NVB | NVB | NM | NB | Z | PS |
| **NS** | NB | NM | NB | NS | Z | PS | PM |
| **Z** | NB | NM | NS | Z | PS | PM | PB |
| **PS** | NM | NS | Z | PS | PB | PB | PB |
| **PM** | NS | NS | PB | PM | PB | PVB | PVB |
| **PB** | NS | PS | PB | PB | PVB | PVB | PVB |

### 4.2 Wheel slip control system design

Based on the principle approach in section (3-2), the main objective of the wheel slip controller is to maintain the $l$ in the optimal slip region ($|l| < l_{opt}$). The region is separately defined for each friction coefficient. Thus, the proposed slip controller should be able to maintain $l$ in variable region by considering different road conditions and the sign of the switching function. To reach this goal, a fuzzy controller with a variable input scaling factor is proposed.

In Fig.9 the block diagram of the slip controller system is shown. Slip ratio and its variation are defined as the controller inputs. The output of the controller called "gain updating factor" ($r_i$) which is always between 0 and 1. The rule base of the slip controller is shown in Table 3. It can be easily inferred from the table when the magnitude of the slip ratio becomes large, the gain updating factor becomes small (near zero). By using this procedure, the wheel torque ($T_i$) is moderated before applying to the electric motor to maintain the slip ratio within the optimum region.

The membership function of the slip ratio, change of slip ratio and the updating factor $r$, are depicted in Fig. 10. The optimum region has been highlighted in Fig.10 (a). In order to keep the slip ratio close to its optimum quantity, the membership functions become narrow in this region.

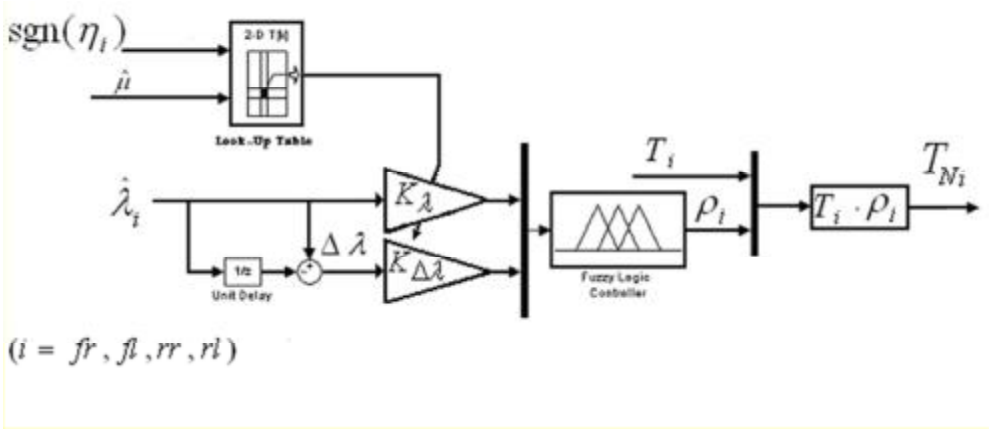


**Fig9.** Wheel slip controller

| $\Delta\lambda$ \ $\lambda$ | NB | NM | NS | Z | PS | PM | PB |
|---|---|---|---|---|---|---|---|
| NB | Z | Z | VS | VS | M | M | Z |
| NM | Z | VS | VS | S | M | M | Z |
| NS | Z | S | M | M | VB | M | Z |
| Z | Z | M | B | VB | B | M | Z |
| PS | VS | M | VB | M | M | S | Z |
| PM | VS | M | M | S | VS | VS | Z |
| PB | VS | M | M | VS | VS | Z | Z |

**Table 3:** Fuzzy Rules for Wheel Slip Controller

The role of $K_l$ in fuzzy logic slip controller system has been shown in Fig .10(a). It can be easily seen that the input scaling factor of $K_l$ and the set of linguistic terms are equivalent to the set of linguistic terms with universe of discourse between $[-\frac{1}{K_l} \quad \frac{1}{K_l}]$. Therefore at any moment, the input scaling factor $K_l$, for each wheel is adjusted on-line according to the sign of the switching function $h_i$ and the estimated friction coefficient of the road $\hat{m}$. The values of $K_l$ are defined in Table 4 based on the optimum wheel slip ratio registered on Table 1 and the sign of the switching function.

The sign of the switching function is a key factor in definition of the input scaling factor. The switching function sign is defined according to wheel slip angle and the controller output. During the maneuver the switching function sign variation is continuously possible due to noise contaminations.

## 5. Simulation and evaluation of the control system

In this section, computer simulations are conducted to evaluate the control systems. For this purpose the vehicle response is evaluated on the basis of lane change and slalom maneuvers. After the close examination of the system response from different aspects, we can make an appropriate decision. The principal approach in this paper is the optimal tire lateral force usage in controlling the vehicle yaw rate which is considered as the main factor in the simulation process.

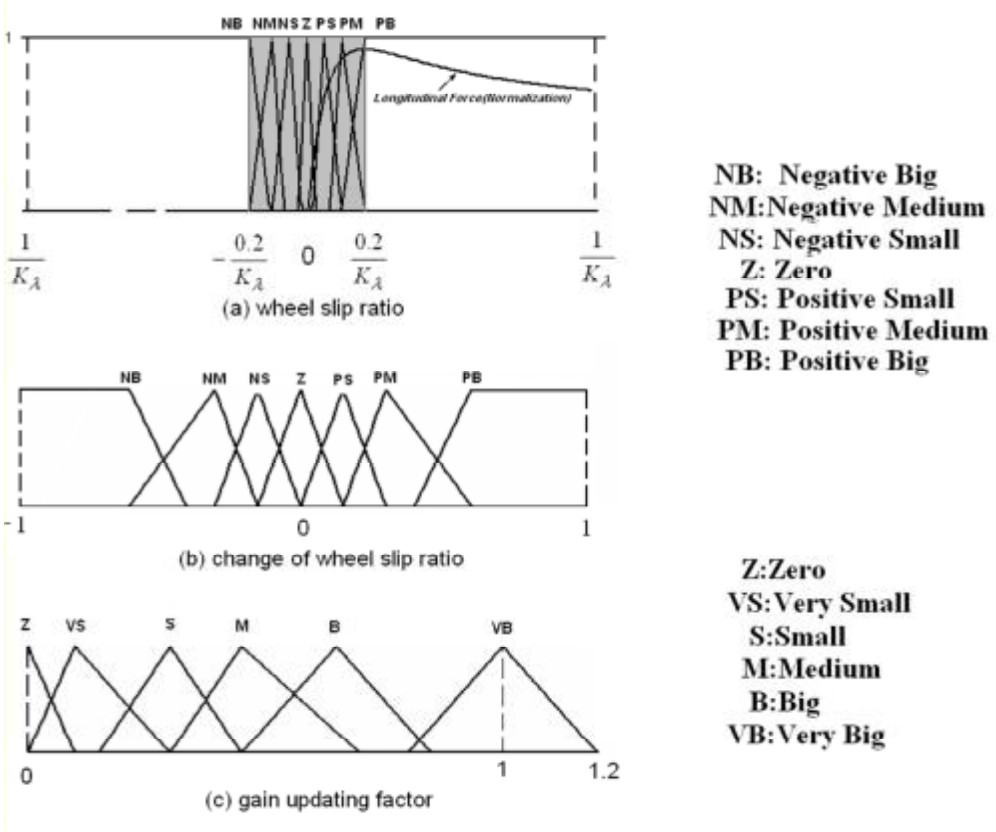


**Fig10.** Membership function of (a) $l$ , (b) $\Delta l$ , (c) $r$

*3-a Front Wheels slip controller*

| $\hat{m}$ <br> $h$ | 0.1 | 0.2 | 0.3 | 0.4 | 0.5 | 0.6 | 0.7 | 0.8 | 0.9 | 1 |
|---|---|---|---|---|---|---|---|---|---|---|
| $h \geq 0$ | 1 | 1 | 1 | 1 | 1 | 1 | 1 | 1 | 1 | 1 |
| $h < 0$ | 10 | 6.6 | 5 | 4 | 3.3 | 2.85 | 2.5 | 2 | 1.8 | 1.67 |

*3-b Rear Wheels slip controller*

| $\hat{m}$ <br> $h$ | 0.1 | 0.2 | 0.3 | 0.4 | 0.5 | 0.6 | 0.7 | 0.8 | 0.9 | 1 |
|---|---|---|---|---|---|---|---|---|---|---|
| $h \leq 0$ | 1 | 1 | 1 | 1 | 1 | 1 | 1 | 1 | 1 | 1 |
| $h > 0$ | 10 | 6.6 | 5 | 4 | 3.3 | 2.85 | 2.5 | 2 | 1.8 | 1.67 |

**Table 4.** Input Scaling Factor on different road friction coefficient and positive/negative switching function

### 5.1. Lane change maneuver on a slippery road

In this maneuver, the vehicle runs with the initial speed of 80 kilometers an hour on a completely slippery road and then at the first second, steer angle is applied as shown in Fig.11. The road friction coefficient is around 0.2 which is assumed accessible for the control system. In Fig.11, vehicle yaw rate and side slip angle response are shown. The figure indicates the control system performance in desired yaw rate tracking while the uncontrolled vehicle responds in an unstable maneuver. Furthermore, in the controlled situation, side slip angle is remarkably limited; though it is a little bit far from its desired value which is usually defined as zero value. We are making an attempt to adjust the side slip angle using another appropriate control input.

The strategy offered in this paper has played a significant role in tracking the desired Yaw rate which is to be confirmed as we move on:

According to Fig.12, the applied torque to the wheels is both appropriate in shape and has an accessible amount. The maximum required torque which does not go beyond 250 N.M can be provided by common actuators. It is clear that both driving and braking torques are used to generate the CYM. Consequently, both traction and braking forces are developed on wheels. This task can be performed by using electric motors on wheels to generate individual wheel torque.

In Fig.13, the meaningful variations of the very important quantity of this paper; that is the scaling factor is shown. Considering the factors influencing the definition of this quantity and the fact that the main part of the maneuver is done between the first to third seconds, we can justify that the system diagnoses the decreasing effect of the front wheel lateral forces on CYM. Input scaling factor has the least possible amount; that is one. Based on the same process, we can recognize the increasing effect of the rear wheel lateral force on CYM.

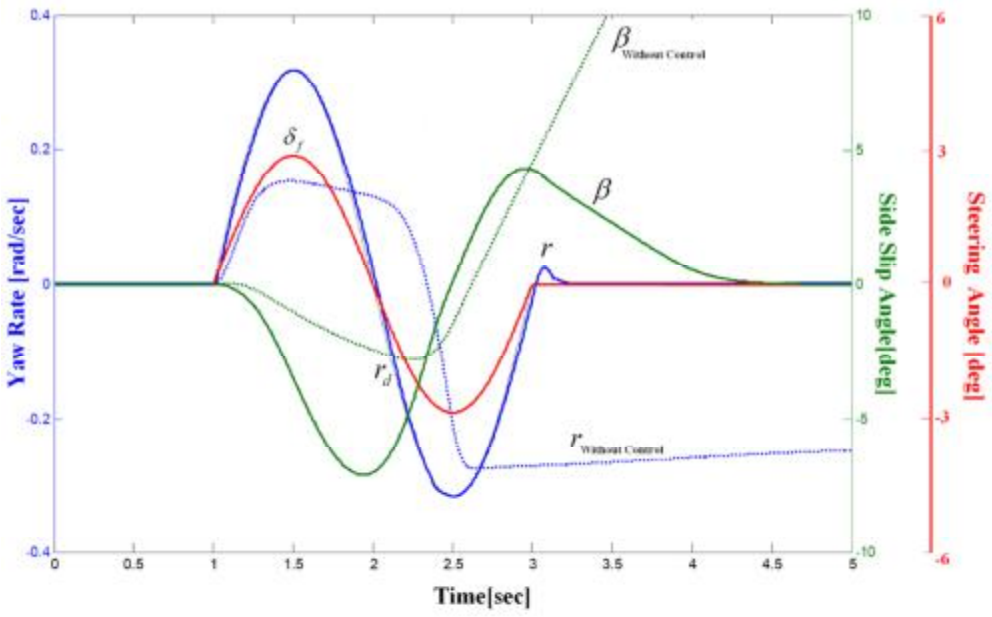


**Fig11.** Yaw Rate and side slip angle response

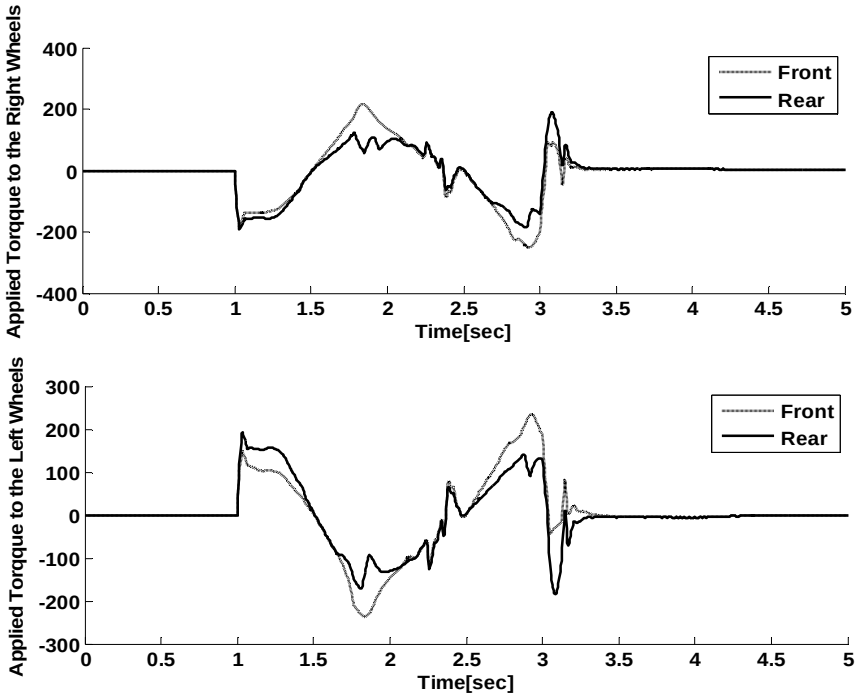


**Fig12.** Applied torque to the wheels

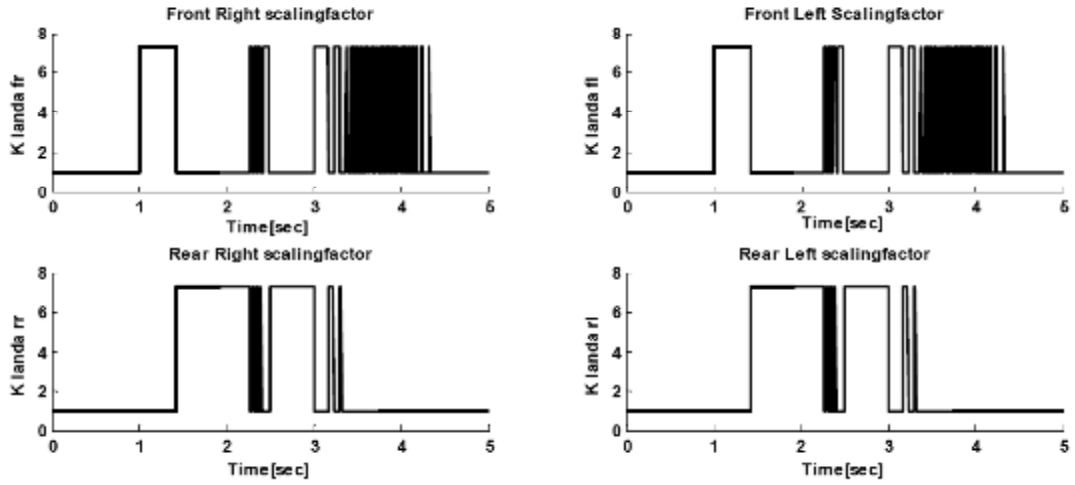


**Fig13.** Input scaling Factor of slip controllers

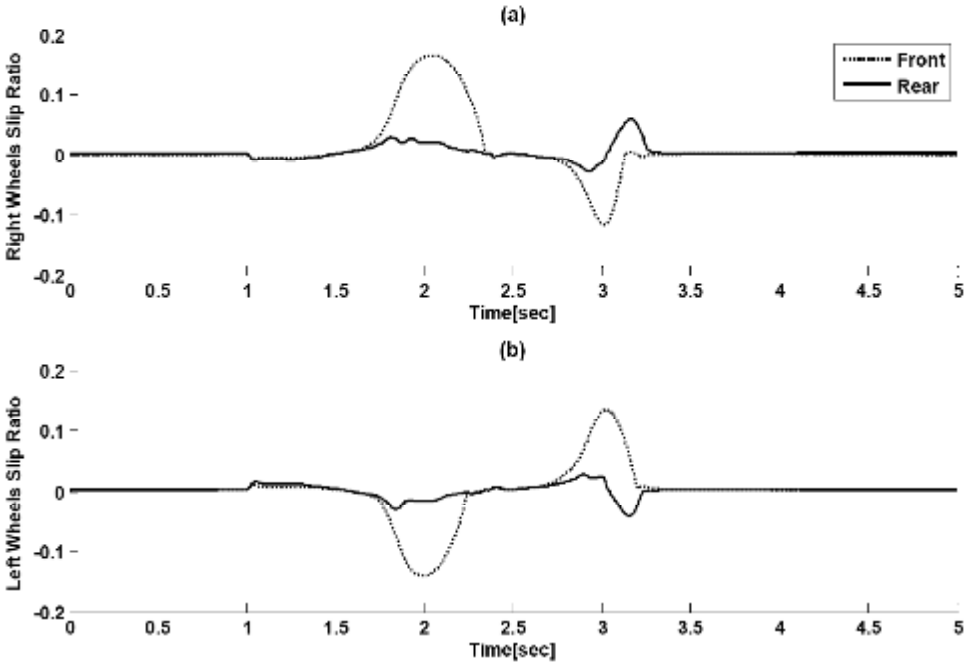


**Fig14.** Slip ratio of wheels

In Fig. 14, the direct effect of the scaling factor variation on the permitted region of slip ratio is clearly observed. The front wheel slip ratio is permitted to go up to 0.2 so that the related lateral forces are reduced to the most possible amount and their negative effects are decreased. The rear wheels function in a reverse manner. In these wheels, wheel slip scaling factor increase to 7 to maintain the wheel slip in narrow band (That is $\frac{0.2}{7}$). Furthermore, the wheel lateral forces are optimally used.

It is necessary to make a comparison to understand the continuous variation effects on the system performance in a better way. Therefore, the proposed systems response is evaluated against two systems with fixed scaling factors. According to Fig. 14, input scaling factor varies between 1 to 7. So for system Type (1), the input scaling factor for all wheels is supposed to be 7 and for system Type (2) it is supposedly 1.

In Fig. 15 the response of these two control approaches in tracking desired Yaw rate is shown. We can observe that in the first part of the maneuvers, the desired yaw rate tracking is satisfactory conducted. However, at the beginning of the second part of the maneuver both approaches failed to track the desired value. The wheel slip ratio and tire lateral force in these three approaches are shown in Fig 16. In system Type (2), the slip ratio of each wheel is permitted to increase by 0.2 while in system Type (1), the slip for all the wheel is restricted in a narrow band because of the rather large scaling factor. The effect of the slip ratio variations on tire lateral forces has been clearly shown. The proposed algorithm has diagnosed the negative effects of the front wheel lateral forces on the CYM generation in some parts of the maneuver. It has also allowed then to be saturated. On the other hand in system Type (1), the four wheel lateral forces are maintained as reflecting the selected input scaling factor while in system Type (2) four wheel lateral forces are saturated.

The points made before are confirmed through the comparison of the three approaches in the yaw moment generation. In Fig. 17, the generated Yaw moment of the lane change maneuver is compared in the three new approaches. In the proposed approach, in critical situation, the vehicle has been able to generate greater yaw moment than the Type1,2 while they all have the same dynamic capacity. In Fact, the main reason for the failure of systems Type 1 and Type 2 in pursuing desired yaw rate is the shortage in generating sufficient Yaw moment. However the proposed approach has succeeded in satisfying the desired control requirement through the application of all the dynamic capacities.

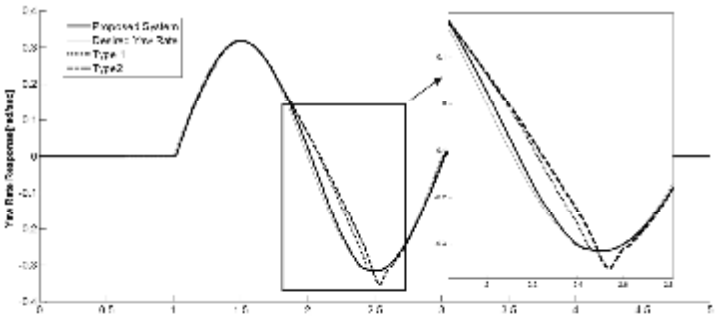

**Fig15.** Yaw rate response for 3 mentioned approaches

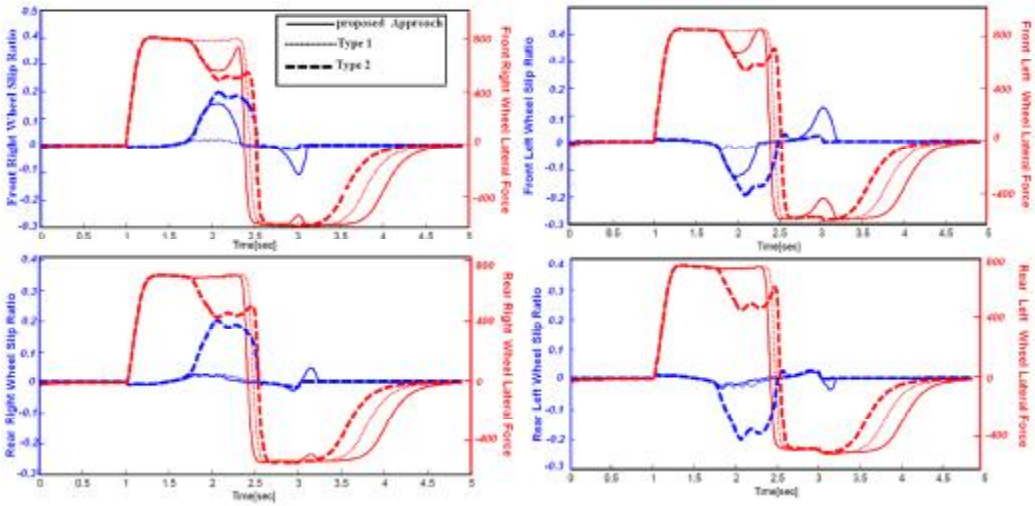


**Fig16.** Slip ratio and lateral force of wheels

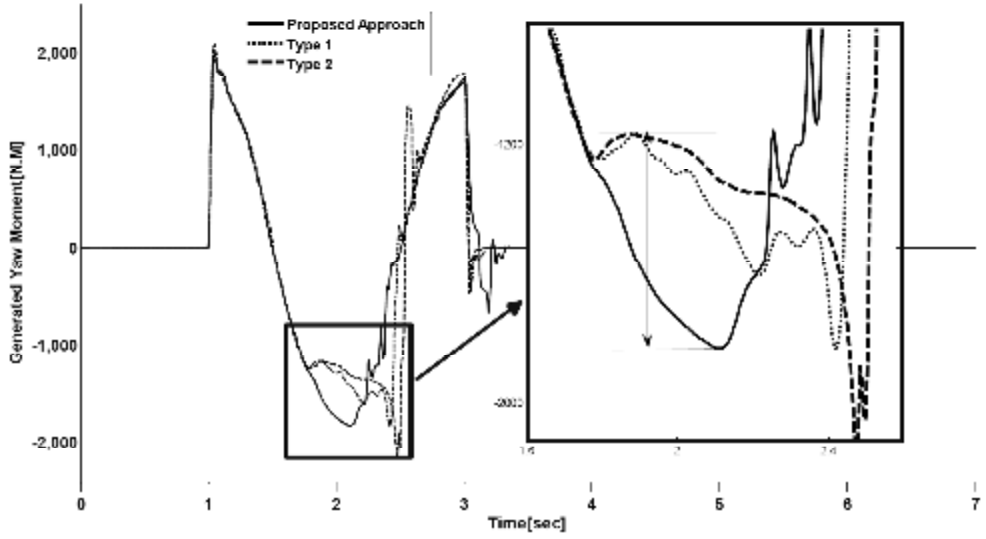


**Fig17.** Generated yaw moment by proposed DYC and Type 1,2

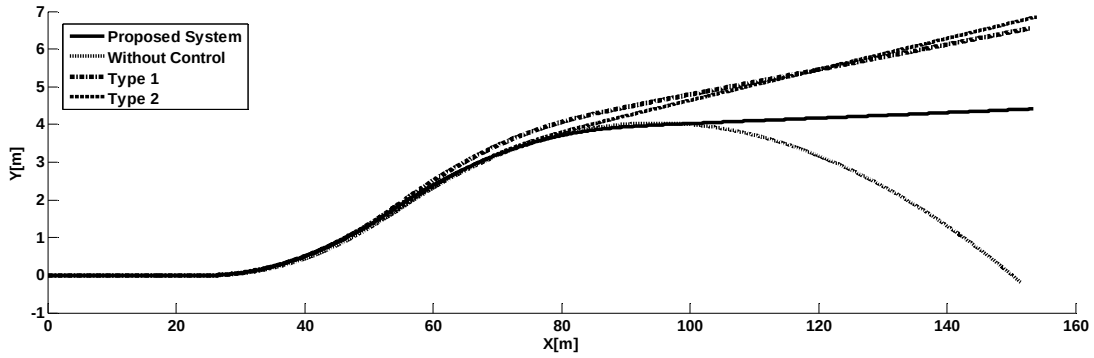


**Fig18.** Vehicle trajectory

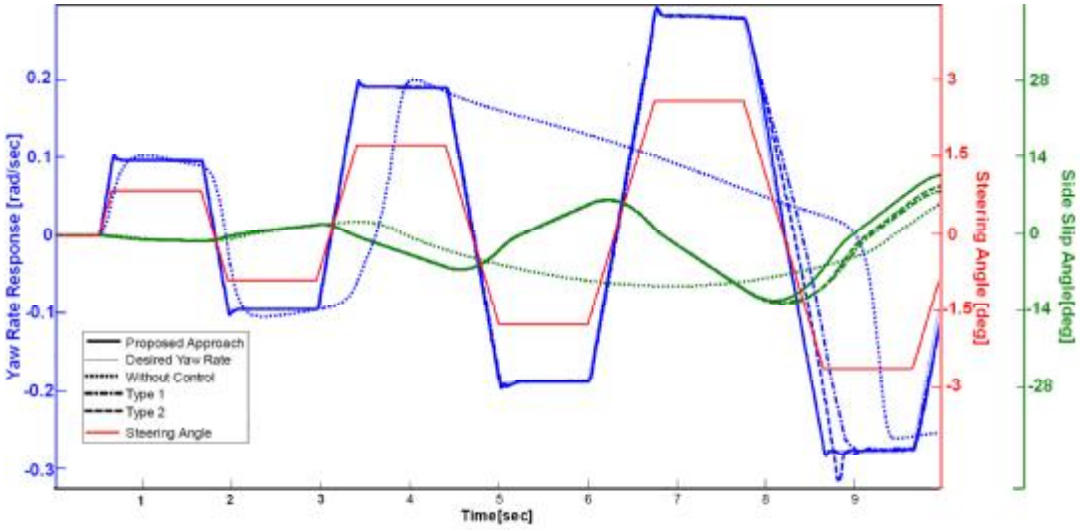


**Fig19.** Vehicle responses at the slalom maneuver

Fig. 18 indicated the path of the vehicle in the lane change maneuver. The vehicle has been guided in the appropriate path using the proposed approach. In approach Type 1 and 2 it is necessary for the driver to make a lot of effort to return the vehicle to the desired path.

### 5.2 slalom maneuver on slippery roads

This maneuver resembles the previous one in terms of conditions. The vehicle runs with the speed of 80 kilometers per hour and then the steer angle whose curve is shown in Fig.18 applied at the first second. In Fig.19, the desired yaw rate tracking of the four situations without control, the proposed approach and systems Type 1 and 2 have been compared. In the initial parts of the maneuver all three approaches, have tracked the desired yaw rate, but at the end of the maneuver the system require a larger yaw moment. In this case, only the proposed approach has been able to track the desired value appropriately.

In Fig.20 wheel slip ratio and Lateral tire force have been compared for the three approaches. Wheel slip ratios are almost the same to the end of the maneuver, but at the end of the maneuver some differences arise. As expected, in physical limit of adhesion, slip ratio of Type2 is permitted to grow up to the bound of the stable region while slip ratio of Type 1 is imprisoned in a narrow region. The slip ratio related to the proposed approach is constantly maintained in the appropriate region. In fact these two new figures imply that the proposed approach shows more capabilities as the maneuvers gets harder. In the physical limit of adhesion, it seems that the front wheel lateral force have a negative effect on the CYM. The proposed approach recognizes the event

and allows the wheel slip ratios to go up. Thus, the front wheel lateral forces are saturated and their negative effects on the CYM are mitigated

All the facts are confirmed through the comparison of the generated CYM in the three control approaches. According to Fig.21, at the final period of the maneuver the proposed approach has generated a greater yaw moment than the conventional approaches and therefore comes up with a move appropriate desired yaw rate.

### 5.3. The improvement of the control system based on the simulation results

In the two previous sections, the proposed approach was evaluated in two rather hard maneuvers and it was confirmed. However this approach has two weak points as follows:

A- It is required to define the friction coefficient of the road in the proposed approach. The estimation of road friction coefficient is an expensive and complicated process. The friction coefficient estimation depends on the side slip angle determination of the vehicle. Measuring the side slip angle is carried out through GPS based sensors or development of another estimator both of which add to the expense and complexity of the control system.

B- In the proposed approach, switching function was introduced, whose positive or negative sign is a key factor in defining the input scaling factor. The switching function sign is defined according to wheel slip angle sign and the controller output. Furthermore, the estimated friction coefficient amount has an effect on the scaling factor from a quantitative viewpoint. During the maneuver the switching function sign variation is continuously possible and the estimated friction coefficient is contaminated with noise and disturbances. As a result the possibility of chattering input scaling factor is constantly existent. From a practical point of view, this is a remarkable weak point which must be corrected.

The control system is modified as improving the mentioned weak points and on the basis of the simulation results as discussed in the previous section. Some graphs in simulations section help us in the creation of new control system with simpler structures. As in Fig.16 and Fig.20, in lane change, slalom maneuver, the rear wheel slip ratio of the proposed system is willing toward Type 2. The front wheel slip ratio is also willing toward Type 1. The wheel lateral force variations also follow the same pattern in the three control approaches. So, we can hypothesize that:

"The front wheel lateral forces constantly decrease the CYM during different maneuvers. On the contrary, the rear wheel lateral forces increase the CYM as the same time".

To improve the proposed systems, we should omit the switching function from the control system. Taking the importance of the complete usage of dynamic capacity on slipping roads into account, we can define the input scaling factor for the front and rear wheels as 1 and 7 respectively as the fixed values. Once more, we conduct the lane change maneuver using the 2nd proposed system to compare its results with the previous ones. According to the Fig.22, we can see that the second proposed system is successful in tracking the desired Yaw rate and its response equals the first proposed system. The generated CYM is also equal for two control approaches.

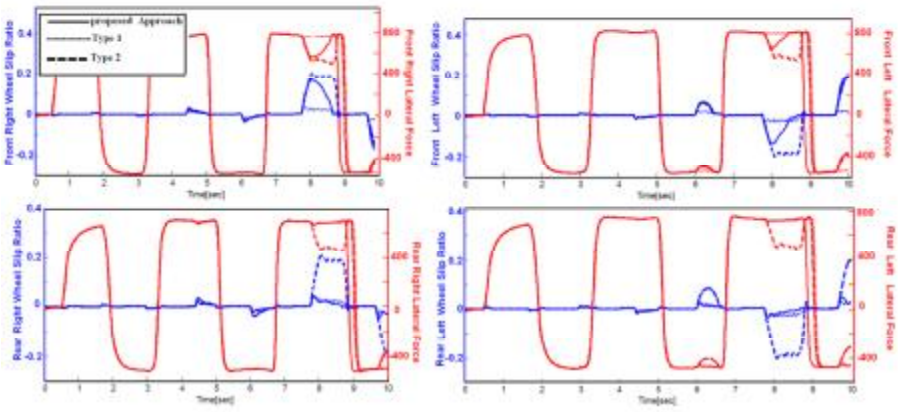


**Fig20.** Wheel slip ratios responses

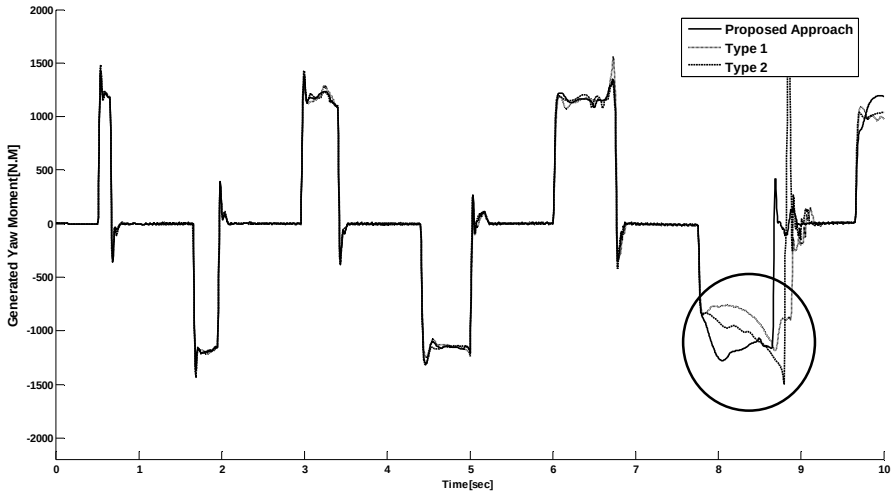


**Fig21.** Generated yaw moment by proposed DYC and Type 1, 2

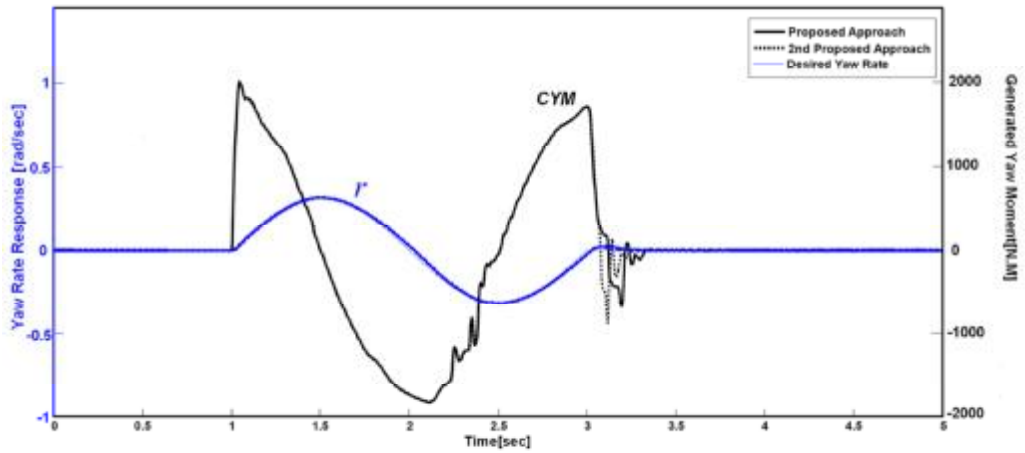


**Fig22.** Vehicle Yaw rate response and generated Yaw moment for the 2nd proposed approach

### 5.4 Single lane change maneuver at the presence of the driver

The difference between this maneuver and the previous ones is the consideration of the driver dynamics while driving. The model presented in the section 2 is used for this purpose. The desired path for the single lane change test is shown in Fig.23. The vehicle runs with the speed of 80 kilometer per hour on a snowy road. As shown in Fig.23, the vehicle motion without control seems completely unstable. On the contrary, the proposed control system stabilizes the vehicle motion and driver simply guides the vehicle in the desired path.

In Fig. 24 vehicle responses are compared in control and without control situations. In both situations the positive control system effects on the vehicle behavior are clearly observed. Not only does DYC system control the vehicle behavior, but it also plays an important role in reducing the driver's physical activities. This is reflected in Fig.24. The driver applies a smaller and more moderated steer angle than the uncontrolled situation as the control system is added.

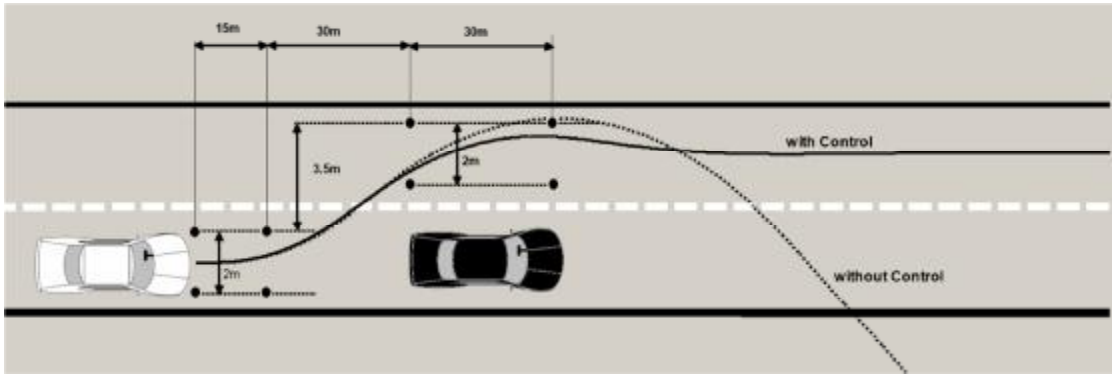


**Fig23.** Desired path for single lane change and vehicle path

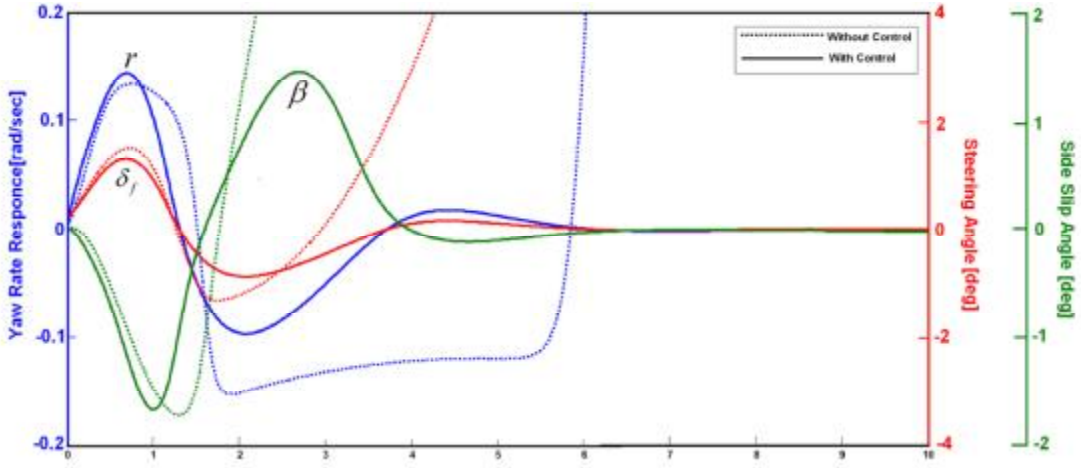


**Fig24.** Vehicle responses in single lane change maneuver

## Conclusion

The optimal usage of lateral forces in yaw rate controlling has been examined in this paper. The proposed control system aimed at maximizing the Control Yaw Moment (CYM) through consideration of lateral forces effect on CYM. Specifically, the following have been achieved in this paper:

A switching function to recognize the positive or negative effect of each wheel lateral force on CYM has bee introduced. The sign of the switching function has been defined for the slip controller to maintain the slip ratio in a region where the CYM can be maximized. The significant improvement of the control system in tracking the desired yaw rate has been shown in the simulation section.

Two weak points of the control system have been recognized. Then, based on the weak points, the control system has been modified to provide a simpler and more applicable structure.

The control system has been also evaluated at presence of the developed driver model in a single lane change maneuver. The simulation results show that not only the system controls the vehicle behavior, but it also plays an important role in reducing the driver's physical activities.

**Notations**

| | |
|---|---|
| $C_{si}$ | Damping coefficient of Suspension |
| $C_{ti}$ | Damping coefficient of tire |
| $fr$ | Front right wheel |
| $fl$ | Front Left wheel |
| $rr$ | Rear right wheel |
| $rl$ | Rear Left wheel |
| $F_{ni}$ | Tire normal force |
| $F_{xi}$ | Tire longitudinal force |
| $F_{yi}$ | Tire lateral force |
| $F_{zi}$ | Suspension force applied to unsprung mass |
| $F_{zti}$ | Tire force applied to unsprung mass |
| $g$ | Gravity acceleration |
| $h$ | Height of CG |
| $I_{xx}$ | Moments of inertia of total Vehicle about X axis |
| $I_{yy}$ | Moments of inertia of total Vehicle about Y axis |
| $I_{zz}$ | Moments of inertia of total Vehicle about Z axis |
| $I_{sxx}$ | Moments of inertia of sprung mass about X axis |
| $I_{syy}$ | Moments of inertia of sprung mass about Y axis |
| $I_{szz}$ | Moments of inertia of sprung mass about Z axis |
| $I_w$ | Moments of inertia of wheels |
| $K_{si}$ | Spring constant of Suspension |
| $K_{ti}$ | Spring constant of tire |
| $K_{us}$ | Understeer gradient |
| $L_{f,r}$ | Distance of the CG from Front/Rear axle |
| $L$ | Vehicle wheel base |
| $m_s$ | Sprung mass |
| $m_t$ | Vehicle total mass |
| $m_{ui}$ | Unsprung mass |
| $M_{zi}$ | Tire self-aligning torque |
| $p$ | Roll rate |
| $q$ | Pitch rate |
| $r$ | Yaw rate |
| $R_{eff}$ | Effective radius of wheel |
| $SL_i$ | Static load of tire |
| $T_f, T_r$ | Front and Rear Track width |
| $T_{Ni}$ | Applied torque to the wheel |
| $T_{pedal}$ | Driving or braking torque applied by the driver |
| $u$ | Longitudinal velocity |
| $v$ | Lateral velocity |
| $y$ | Vehicle lateral displacement |
| $y_d$ | Desired path |
| $y_e$ | Deviation from the desired path |
| $d_i$ | Vertical displacement of the wheels |
| $w$ | Vertical velocity |
| $Z_{CG}$ | Vertical displacement of CG |
| $Z_i$ | Vertical displacement of sprung mass corner |
| $Z_{ui}$ | Unsprung mass displacement |
| $Z_{si}$ | Height variation of Ground surface |
| $a_i$ | Wheel slip angle |
| $\Delta T$ | Yaw rate controller output |
| $d_f$ | Front steering angle |
| $j$ | Roll angle |
| $h_i$ | Switching function |
| $l_i$ | Wheel slip ratio |
| $m$ | Friction coefficient of road |
| $q$ | Pitch angle |
| $w_i$ | Rotational speed of wheel |

## Acknowledgment

A part of this work was supported by South Tehran Branch, Islamic Azad University under Project A New combination Control System is including Active Steering and Active Braking in passenger vehicle

**References**


[1]. S. Matsumoto, H. Yamaguchi, H. Inoue, Y. Yasuno, Braking force distribution control for improved vehicle dynamics, Proceedings of AVEC ’92, Yokohama, Japan, (1992).

[2]. A.T. Van Zanten, K. Erhardt, G. Pfaff, VDC, The vehicle dynamics control system Of Bosch, SAE paper No.950759, (1995).

[3]. Nam, Kanghyun, Hiroshi Fujimoto, and Yoichi Hori. "Lateral stability control of in-wheel-motor-driven electric vehicles based on sideslip angle estimation using lateral tire force sensors." Vehicular Technology, IEEE Transactions on 61.5 (2012): 1972-1985.

[4]. Hsiao, Tesheng. "Direct longitudinal tire force control under simultaneous acceleration/deceleration and turning." American Control Conference (ACC), 2013. IEEE, 2013.

[5]. Hsiao, Tesheng. "Robust Estimation and Control of Tire Traction Forces." Vehicular Technology, IEEE Transactions on 62.3 (2013): 1378-1383.

[6]. S. Anwar, Generalized predictive control of yaw dynamics of a hybrid brake-by-wire equipped vehicle, Mechatronics, 15, (2005) 1089-1108.

[7]. M. Canale, L. Fagiano, P. Milanese, P. Borodani, Robust vehicle yaw control using active differential and internal model control, Proceeding of the 2006 American Control Conference, Minneapolis, Minnesota, USA, (2006).

[8]. S. Inagaki, I. Kshiro, M. Yamamoto, Analysis on vehicle stability in critical cornering using phase-plane method, Proceedings of AVEC ’94, Tsukuba, Japan, (1998).

[9]. M. Abe, Y. Kano, K. Suzuki, Y. Shibahata, Y. Furukawa, Side-slip control to stabilize vehicle lateral motion by direct yaw moment, Jap. Soc. Automot. Engre. Rev., (2001) 413-419.

[10]. M. Shino, M. Nagai, Yaw-moment control of electric vehicle for improving handling and stability, Jap. Soc. Automot. Engre . Rev., (2001) 473-480.

[11]. A. Goodarzi, E. Esmailzadeh, Design of a VDC system for all-wheel independent drive vehicles, IEEE/ASME Trans. Mech., 12 (2007) 632-639,

[12]. Tavasoli, Ali, Mahyar Naraghi, and Heman Shakeri. "Optimized coordination of brakes and active steering for a 4WS passenger car." ISA transactions 51.5 (2012): 573-583.

[13]. Doumiati, Moustapha, et al. "Gain-scheduled LPV/Hinf controller based on direct yaw moment and active steering for vehicle handling improvements." Proceedings of the 49th IEEE Conference on Decision and Control (CDC 2010). 2010.

[14]. D. Kim, S. Hwang, H. Kim, Vehicle stability enhancement of four-wheel-drive hybrid electric vehicle using rear motor control," IEEE Trans. Veh. Technol., 57 (2008) 727-735.

[15]. M. Nagai, M. Shino, F. Gao, Study on integrated control of active front steer angle and direct yaw moment, Jap. Soc. Automot. Engre. Rev., (2002) 309-315.

[16]. J. Song, Integrated control of brake pressure and rear-wheel steering to improve lateral stability with fuzzy logic. International Journal of Automotive Technology, 2012, 13(4), 563-570.

[17]. B. Mashadi, B., Majidi, M, Integrated AFS/DYC sliding mode controller for a hybrid electric vehicle. International Journal of Vehicle Design, 2011, 56(1), 246-269.

[18]. Doumiati, Moustapha, et al. "Integrated vehicle dynamics control via coordination of active front steering and rear braking." European Journal of Control 19.2 (2013): 121-143.

[19]. H. Peng, J.S. Hu, Traction/braking force distribution for optimal longitudinal motion during curve following, Veh. Syst. Dyn., 26, (1996) 301-320.

[20]. Tavasoli, Ali, and Mahyar Naraghi. "Interior-Point Method to Optimize Tire Force Allocation in 4-Wheeled Vehicles Using High-Level Sliding Mode Control with Adaptive Gain." Asian Journal of Control 15.4 (2013): 1188-1200.

[21]. H.B. Pacejka, Tyre and vehicle dynamics, Oxford: Butterworth Heinemann, (2002).

[22]. A. Renski, Identification of driver model parameters, Inter.J. Occupational Safety and Ergonomics, 7 (2001) 79–92.

[23]. J.G. Gerdes, E.J. Rossetter, A unified approach to driver assistance system based on artificial potential fields, Journal of Dyn. Sys., Meas., and Control, 123 (2001) 431–438.

[24]. T. Mansour, PID Control, Implementation and Tuning,, Publisher: InTech, Chapters published April 19, 2011 under CC BY-NC-SA 3.0 license

[25]. F. Tahami, R. Kazemi, S. Farhanghi, A novel driver assist stability system for all-wheel-drive electric vehicles, IEEE Trans. Veh. Technol., 52 (2003) 683-692.